Dendrimers Functionalized with a Single Pyrene Label: Synthesis, Photophysics, and Fluorescence Quenching

Claudia M. Cardona,[†] Tom Wilkes,[†] Winston Ong,[†] Angel E. Kaifer,[†] Tracy Donovan McCarley,[‡] Siddarth Pandey,[§] Gary A. Baker,[¶] Maureen N. Kane,[¶] Sheila N. Baker,[¶] and Frank V. Bright[¶,*]

Center for Supramolecular Science and Department of Chemistry, University of Miami, Coral Gables, Florida 33124-0431, Choppin Laboratories of Chemistry, Louisiana State University, Baton Rouge, Lousiana 70803-1804, Department of Chemistry, New Mexico Institute of Technology, Socorro, New Mexico 87801, and Department of Chemistry, Natural Sciences Complex, University at Buffalo, The State University of New York, Buffalo, New York 14260-3000

Received: April 2, 2002; In Final Form: June 10, 2002

We have used a wide variety of molecular (i.e., nitromethane, acrylamide, *N*,*N*′-dimethylaniline, and methyl iodide) and ionic (iodide and cupric ions) quenchers to assess the relative structural permeabilities of a single, pyrenyl residue attached to the tertiary amine within a series of asymmetric poly(amido) dendrimers possessing carboxylate moieties at their periphery. From these quenching experiments, chain segmental densities and pyrene accessibility are probed as a function of dendrimer generation number (**P*n***, $n = 1$, 2, or 3), providing insight into the roles of size and electrostatics in this process. With the exception of dendrimer quenching by Cu^{2+}, we observe classic Stern−Volmer behavior for **P*n*** fluorescence quenching by all quenching agents. The recovered Stern−Volmer quenching constants (K_{SV}) and bimolecular quenching rates (k_q) generally decrease as *n* increases. This result is explained by a blocking of the pyrenyl residue by the growing dendrimer network. The decrease is particularly dramatic for the anionic heavy atom quencher I^-. This observation is rationalized in terms of pronounced electrostatic repulsion between the I^- quencher and the terminal COO^- residues of the dendrimer combined with an increase in the molecular network density surrounding the pyrenyl moiety as *n* increases. The Cu^{2+} quenching of the dendrimers is inconsistent with a diffusion-controlled reaction. Binding between the dendrimer and the Cu^{2+} is demonstrated.

Introduction

Research on functionalized dendrimers has flourished during the past few years.[1] One of the most important reasons driving this extensive research work is that the attachment of functional 'probes' to these macromolecular structures facilitates the detailed investigation of their properties. In this regard, pyrene is an obvious choice as a probe because its fluorescence properties are well-known and strongly dependent on the microenvironment.[2] Therefore, the noncovalent incorporation of pyrene into the cavities present inside dendrimers has received some attention, as illustrated by recent work reported by the Malliaris−Paleos group.[3] A different approach relies on the covalent attachment of pyrene residues to dendrimers. For instance, Frank et al. investigated the properties of pyrene-labeled arborescent polystyrenes.[4] Baker and Crooks prepared and studied a series of poly(propylene imine) dendrimers functionalized with multiple, peripheral pyrene groups.[5] As we were completing our own investigation, the groups of Shapiro and Hanson reported the synthesis, characterization, and photophysics of pyrene-labeled poly(aryl ether) monodendrons.[6] Fréchet and co-workers have also recently reported star polymers with a pyrene core.[7]

Our work in this area has focused on dendritic molecules built through the covalent attachment of a single functional group to dendritic building blocks inspired by the work of Newkome and co-workers.[8] The resulting unsymmetric dendrimers have the functional group or probe attached "off center", that is, at the first branching point in these macromolecules.[9,10] In this paper, we report the synthesis of a new series of water-soluble, pyrene-labeled dendrimers (first, second, and third generation, see Figure 1), as well as their photophysical and quenching properties.

Experimental Section

Reagents for Synthesis. All chemicals were reagent grade (Aldrich, Sigma, or Fisher) and were used as received. Tetrahydrofuran (THF) was freshly distilled over sodium. Column chromatography was performed with Scientific Adsorbents silica gel (63−200 μm).

3 Cascade: 3-(1-Pyrenyl)-propane [1]: (3-Oxo-2-azapropyldyne): Propanoic (P1). 4-(1-Pyrenyl)butanoic acid (0.206 g, 0.714 mmol) was dissolved in 3.6 mL of 0.2 M NaOH. The water was removed under vacuum and the salt was completely dried in a vacuum oven at 100 °C. The sodium salt was then stirred under N_2 in 50 mL of dry benzene and 10 mL of oxalyl chloride at room temperature was added for an hour. After complete removal of the excess reagent and the solvent under reduced pressure, the residue was stirred with Behera's amine[8] (0.320 g, 0.771 mmol) and Et_3N (0.15 mL, 1.1 mmol) in 25

* Corresponding author. E-mail: chefvb@acsu.buffalo.edu.
[†] University of Miami.
[‡] Louisiana State University.
[§] New Mexico Institute of Technology.
[¶] University at Buffalo.

10.1021/jp020862h CCC: $22.00
Published on Web 08/06/2002

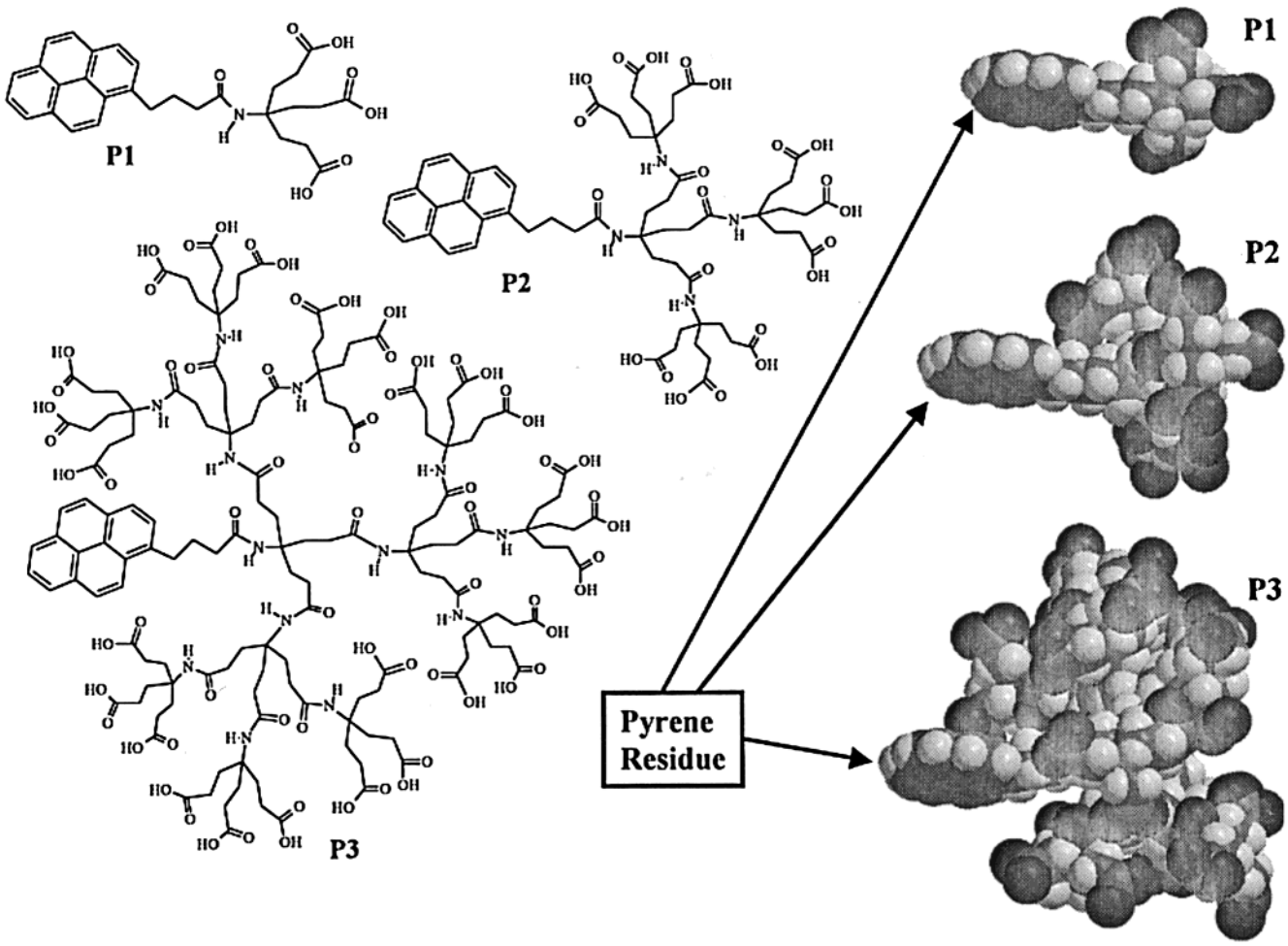

Figure 1. Chemical structures of the dendrimers studied (left) and space-filling structures after using the SYBYL force field (right).

mL of dry THF for 4 days under N_2 at room temperature. Purification of the obtained greenish-brown residue was accomplished by column chromatography (SiO_2, 2:1 CH_2Cl_2/EtOAc) to produce the lipophilic (*tert*-butyl ester) form of the dendrimer (0.380 g, 78%). The obtained beige product was hydrolyzed (0.190 g, 0.278 mmol) by stirring it in 10 mL of 96% formic acid for 15 h. After removal of the formic acid, the residue was washed with hot hexane and filtered, and a beige powder, **P1** (0.136 g, 95%), was obtained after drying in a vacuum oven at 100 °C overnight. Fourier transform (FT)-IR (KBr): 1716 [ν(C═O)] cm^{-1}; 1652 [ν(AMIDE I, C═O)] cm^{-1}; 1540 [ν(AMIDE II)] cm^{-1}; 1286 [ν(C−O)] cm^{-1}. ^{1}H NMR (DMSO-d_6): δ 1.75−2.20 (m, CH_2CH_2, 12 H); 1.971 (q, CH_2, 2H, J = 7.7 Hz); 2.234 (t, CH_2, 2H, J = 7.1 Hz); 3.289 (t, CH_2, J = 8 Hz); 7.268 (bs, NH, 1H); 7.9−8.4 (m, pyrCH, 9H); 12.07 (bs, COOH, 3H). ^{13}C NMR (DMSO-d_6): δ 27.680 (CH_2); 28.139, 29.080 (CH_2CH_2); 32.228 (CH_2); 35.574 (CH_2); 56.376 [$C(CH_2CH_2)_3$]; 123.392, 124.097, 124.681, 124.837, 126.028, 126.407, 127.162, 127.378, 128.084, 129.226, 130.367, 130.826, 136.543 (pyrene); 172.022 (CONH); 174.392 (COOH). [λ_{abs}^{max}, nm (ϵ, 10^4 M^{-1} cm^{-1}), phosphate buffer pH 7]: 342.0 (3.7). Matrix-assisted laser desorption ionization-time of flight (MALDI-TOF) MS (neat): 517.856 (M^+, M calcd 517.58).

9 Cascade: 3-(1-Pyrenyl)-propane [1]: (3-Oxo-2-azapropylidyne): (3-Oxo-2-azapentylidyne): Propanoic (P2). 4-(1-Pyrenyl)-butanoic acid (0.100 g, 0.347 mmol) was again converted to the sodium salt as described above. The anhydrous salt was stirred in 50 mL of dry benzene and 10 mL of oxalyl chloride for an hour. The solvent was then removed completely, and the residue was stirred with the second-generation analogue of Behera's amine[9] (0.522 g, 0.362 mmol) and Et_3N (0.10 mL, 0.72 mmol) in 25 mL of dry THF under N_2 for 4 days at room temperature. Purification entailed column chromatography (SiO_2, 2:1 CH_2Cl_2/EtOAc) and a pale yellow powder, the lipophilic dendrimer was obtained (0.313 g, 53%). Hydrolysis of this product (0.211 g, 0.123 mmol) was performed as described above and a beige powder, **P2**, was obtained (0.139 g, 94%). FT-IR (KBr): 1716 [ν(C═O)] cm^{-1}; 1652 [ν(AMIDE I, C═O)] cm^{-1}; 1522 [ν(AMIDE II)] cm^{-1}; 1313 [ν(C−O)] cm^{-1}. ^{1}H NMR (DMSO-d_6): δ 1.7−2.2 (m, CH_2CH_2 gen 2, 36 H); 1.9−2.1 (m, CH_2CH_2 gen 1, 12H); 2.188 (t, CH_2, 2H); 7.228 (bs, NH, 4H); 7.9−8.5 (m, CH, pyrene, 9H); 12.049 (bs, COOH, 9H). ^{13}C NMR (DMSO-d_6): δ 27.540 (CH_2); 28.090, 29.103 (CH_2CH_2 gen 2); 30.263, 30.707 (CH_2CH_2 gen 1); 32.198 (CH_2); 35.680 (CH_2); 56.240 [$C(CH_2CH_2)_3$ gen 2]; 56.759 [$C(CH_2CH_2)_3$ gen 1]; 123.578, 124.139, 124.196, 124.700, 124.780, 124.886, 126.024, 126.377, 127.151, 127.424, 127.614, 128.152, 129.207, 130.434, 130.838, 136.630 (pyrene); 171.532 (CONH gen 1); 172.200 (CONH gen 2); 174.415 (COOH). [λ_{abs}^{max}, nm (ϵ, 10^4 M^{-1} cm^{-1}), phosphate buffer pH 7]: 343.0 (3.3). MALDI-TOF MS (DHB matrix): 1204.91 (M^+, M calcd 1205.28); 921.68 (MH^+ − PyrCOOH).

27 Cascade: 3-(1-Pyrenyl)-propane [1]: (3-Oxo-2-azapropylidyne): (3-Oxo-2-azapentylidyne): (3-Oxo-2-azapentylidyne): Propanoic (P3). The sodium salt of the 4-(1-pyrenyl)-butanoic acid (0.038 g, 0.132 mmol) was again prepared as described above. The anhydrous salt was stirred in 50 mL of dry benzene and 10 mL of oxalyl chloride for an

TABLE 1: Photophysical Parameters of the Pyrene-labeled Dendrimers (P1, P2, and P3) Dissolved in PB

dendrimer	λ_{abs}^{max} (nm)[a]	ϵ ($dm^3\,mol^{-1}\,cm^{-1}$)[b]	Φ_f	$<\tau>_o$ (ns)[c]	k_r ($10^6\,s^{-1}$)	k_{nr} ($10^6\,s^{-1}$)
P1	342.0	3.57×10^4	0.651 ± 0.003	128.9 ± 2.5	5.05 ± 0.10	2.71 ± 0.06
P2	343.0	3.27×10^4	0.698 ± 0.002	137.2 ± 2.5	5.09 ± 0.09	2.20 ± 0.04
P3	344.5	2.16×10^4	0.819 ± 0.002	144.0 ± 2.5	5.69 ± 0.10	1.26 ± 0.03

[a] Imprecision is 1 nm. [b] Imprecision is <5%. [c] $<\tau> = (\Sigma\alpha_i\tau_i^2)/(\Sigma\alpha_i\tau_i)$; for a multiexponential decay scheme.

hour. The solvent was then removed completely and the residue was stirred with the third-generation analogue of Behera's amine[9] (0.507 g, 0.112 mmol) and Et_3N (0.05 mL, 0.36 mmol) in 25 mL of dry THF under N_2 for 7 days at room temperature. Purification entailed column chromatography (SiO_2, 5:1 CH_2Cl_2/EtOAc, 2:1 CH_2Cl_2/EtOAc, and EtOAc) and a pale yellow powder, the lipophilic dendrimer was obtained (0.156 g, 29%). Hydrolysis of this product (0.146 g, 0.0305 mmol) was performed as described above and a beige powder, **P3**, was obtained (0.0980 g, 98%). FT-IR (KBr): 1717 [ν(C═O)] cm^{-1}; 1652 [ν(AMIDE I, C═O)] cm^{-1}; 1541 [ν(AMIDE II)] cm^{-1}; 1286 [ν(C−O)] cm^{-1}. ^1H NMR (DMSO-d_6): δ 1.60−2.35 (m, CH_2CH_2, 156 H); 7.2 (bs, NH, 13H) 7.9−8.4 (m, CH, pyrene, 9H); 12.0 (bs, COOH, 27H). ^{13}C NMR (DMSO-d_6): δ 28.125, 29.095 (CH_2CH_2 gen 3); 30.252, 30.764 (CH_2CH_2 gen 2); 56.338 [$C(CH_2CH_2)_3$ gen 3]; 56.744 [$C(CH_2CH_2)_3$ gen 2]; 172.532 (CONH gen 3); 175.200 (COOH). [λ_{abs}^{max}, nm (ϵ, 10^4 M^{-1} cm^{-1}), phosphate buffer, pH 7]: 344.5 (2.2). MALDI-TOF MS (DHB matrix): 3270.72 (MH^+, M calcd 3268.37); 6532.16 (dimerH^+).

Materials for Photophysical and Fluorescence Quenching Studies. The following chemicals were used as received: 1,4-bis[5-phenyloxazole-2-yl)]benzene (POPOP); sodium hydrogen phosphate heptahydrate, and sodium dihydrogen phosphate monohydrate (J. T. Baker, Inc.); potassium iodide (99.99+%), copper(II) sulfate pentahydrate (99.999%), nitromethane (99+%), acrylamide (99+%), *N*,*N*′-dimethylaniline (redistilled, 99.5%), and iodomethane (99%) (Aldrich Chemical Co.). Water was the solvent. It was distilled in quartz and deionized by using a Barnstead NANOpure II four-stage water purification system until the specific conductivity fell below 0.06 μS cm^{-1}. Most experiments were performed in 100 mM phosphate buffer, pH 7.0 (PB). However, all Cu^{2+}-quenching experiments were performed in distilled−deionized water to avoid precipitation with phosphate anion [$K_{SP} \sim 1.3 \times 10^{-37}$ for $Cu_3(PO_4)_2$].[11a] All stock solutions were refrigerated at 4 ± 2 °C in amber poly(tetrafluoroethylene)-lined borosilicate vials (VWR Scientific).

Instrumentation. ^1H and ^{13}C NMR spectra were recorded on a Varian VXR-400 spectrometer; all the chemical shift (δ) values are reported in ppm. MALDI-TOF MS spectra were recorded with a Bruker proFLEX III MALDI-TOF instrument. All UV-visible spectroscopic measurements were performed in 1-cm^2 quartz cuvettes at 22 °C. Electronic absorbance spectra were recorded on a Shimadzu model 2101 or a Milton Roy model 1201 (Spectronic Instruments) UV-visible spectrophotometer. Static fluorescence experiments were performed with an SLM-AMINCO model 48000 MHF fluorometer (Spectronic Instruments). The excitation and emission spectral band-passes were kept at 4 and 1 nm, respectively. The excitation wavelength was set to 337 nm. All spectra were background corrected by using appropriate blanks. Fluorescence quantum yields were determined by using POPOP dissolved in cyclohexane ($\Phi_s = 0.97$) as a standard.[12] All sample solutions were freeze−pump−thaw degassed at least four times to remove residual O_2.[13]

Time-resolved fluorescence measurements were performed by using an IBH model 5000W SAFE time-correlated single-photon-counting fluorometer. Samples were excited at 337 nm with a N_2-filled flashlamp operating at 40 kHz. The fluorescence was detected under magic angle conditions. An emission monochromator was used for wavelength selection ($\lambda_{em} = 376$ nm, $\Delta\lambda = 8$ nm). The typical time resolution for an experiment was 0.47 ns/channel and we used 1024 total channels within the multichannel analyzer. To avoid pulse pile-up, the count rate at each detector was always <800 Hz. Data were acquired until there were at least 10^4 counts in the peak multichannel analyzer channel. The excited-state fluorescence lifetimes were recovered from the time-resolved intensity decay profiles by using a commercially available nonlinear least-squares software package (Globals Unlimited).

Results and Discussion

Synthesis. The pyrene dendrimers reported here were prepared by using the same general methodology used for the synthesis of structurally related ferrocene-[9] and dansyl-labeled[10] dendrimers. In brief, pyrenebutyric acid was converted to its acid chloride and reacted with the appropriate amine dendrons to produce the lipophilic forms of the dendrimers with 3, 9, or 27 *tert*-butyl esters on their peripheries (first, second, and third generation, respectively). Their hydrolysis with formic acid led to the corresponding hydrophilic forms having 3, 9, or 27 surface carboxylic acid residues. These water-soluble dendrimers were fully characterized using FT-IR, ^1H and ^{13}C NMR spectroscopic data, and their molecular weights were verified by MALDI-TOF mass spectrometry (see Experimental Section).

Steady-State Photophysical Studies. The absorbance maxima (λ_{abs}^{max}) and corresponding molar absorptivities (ϵ) for dendrimers **P1**, **P2**, and **P3** (1 μM) dissolved in PB are summarized in Table 1. A small decrease in ϵ is evident as we progress from dendrimer **P1** to **P2** followed by a more pronounced decrease between **P2** and **P3**. Our recovered ϵ values are in line with values previously reported by others for pyrene and pyrene-labeled macromolecules dissolved in aqueous solution or organic solvents.[14,15] For example, Hara et al. report values of 3.30×10^4 $dm^3\,mol^{-1}\,cm^{-1}$ and 2.13×10^4 $dm^3\,mol^{-1}\,cm^{-1}$ for pyrene dissolved in acetonitrile and 2-propanol, respectively.[14] Similarly, Winnik and co-workers report an ϵ value of 4.5×10^4 $dm^3\,mol^{-1}\,cm^{-1}$ for 4-(1-pyrenyl)butanol dissolved in methanol.[15] These authors also noted that ϵ for pyrene-labeled (hydroxypropyl)cellulose decreases from 4.5×10^4 $dm^3\,mol^{-1}\,cm^{-1}$ to 2.5×10^4 $dm^3\,mol^{-1}\,cm^{-1}$ when the solvent is switched from methanol to water.[15]

The dendrimer fluorescence quantum efficiencies (Φ_f) were determined by using the Parker−Rees method.[16] The recovered values are also collected in Table 1. The Φ_f values parallel the ϵ results and increase in the order **P1** < **P2** ≪ **P3**. Our Φ_f values are also well within the range of values reported by other researchers.[14,17,18] Thus, although the data in Table 1 clearly reflect the environmental influence of the dendritic substituents, the trend is surprising for two reasons. First, one might expect the introduction of amido functionalities near the pyrene residue to enhance the dipolarity surrounding the pyrene residue resulting in a lower Φ_f. Second, aromatic and aliphatic amines are well-known quenchers of aromatic hydrocarbon fluores-

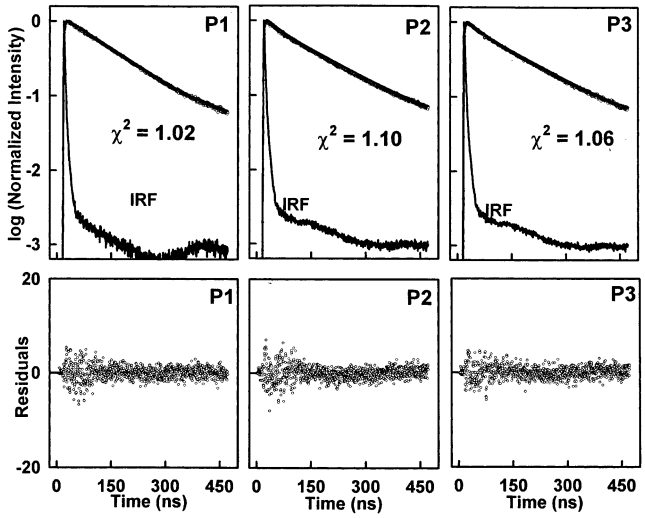

Figure 2. Time-resolved intensity decay traces for **P1**, **P2**, and **P3** dissolved in PB. The instrument response function (IRF), data (points), and fit to triple exponential decay models (—) are shown. The corresponding residuals are shown in the lower panels.

TABLE 2: Parameters Extracted from the Excited-State Fluorescence Intensity Decay of Pyrene-labeled Dendrimers (P1, P2, and P3) Dissolved in PB at 376 nm[a]

dendrimer	τ_1	τ_2	τ_3	α_1/α_2	α_1/α_3	χ^2
P1	127.0					12.8
	127.7	1.0		1.011		1.97
	156.4	115.0	0.3	0.398	0.146	1.02
P2	131.4					15.6
	134.2	6.5		4.252		2.45
	145.0	69.5	0.4	4.631	0.469	1.10
P3	133.2					13.3
	140.9	13.8		2.443		3.40
	144.8	30.9	1.0	35.394	7.068	1.06

[a] All excited-state lifetimes are in nanoseconds. All $<\tau_i>$ and α_i/α_j have imprecisions of 2.5 ns and 0.1, respectively.

cence.[19] As a recent example, Winnik et al. reported that secondary and tertiary amino groups within the actual polymer backbone are responsible for the observed quenching in pyrene-labeled branched polyethylenimines dissolved in aqueous solution; however, the tertiary amines were reportedly far more efficient quenchers.[20] Gauthier and co-workers have also reported a "backbone quenching" effect for highly branched polystyrenes labeled with pyrene relative to the soluble pyrene monomer 1-pyrenemethanol.[4] The results of our experiments demonstrate that these types of "backbone" quenching phenomena are absent in our dendrimers.

Time-Resolved Fluorescence. To further assess the photophysical properties of these dendrimers, we recorded the time-resolved fluorescence intensity decay traces for each dendrimer (Figure 2). In freeze−pump−thaw degassed PB, dilute solutions of each dendrimer ($<1\ \mu$M) exhibited multiexponential intensity decays. On the basis of an assessment of the residuals, auto correlation functions, and χ^2 values, we conclude that **P*n*** intensity decays are well described by a triple exponential decay model (Figure 2, Table 2).

The intensity decay for pyrene when it is attached to another species is often multiexponential.[4,15,21−27] For example, Gauthier and co-workers found that a triple exponential decay model was required to describe the time-resolved intensity decay data for pyrene-labeled arborescent polystyrene.[4] It has also been suggested that the excited-state intensity decay profiles of pyrenyl derivatives bound to *any* macromolecule are multiexponential.[21] This is in striking contrast to the behavior of pyrene dissolved in deaerated water which decays with a single fluorescence lifetime (τ) (175 ns,[22] 200 ± 20 ns,[23] and 200.8 ± 0.9 ns[24]). Similarly, the excited-state fluorescence intensity decay of 1-pyrene butyric acid (PBA) dissolved in toluene is single exponential ($\tau = 61.5$ ns).[25] However, when PBA is incorporated within a silicone film, its intensity decay is no longer single exponential.[25] The Berglund group showed that the time-resolved intensity decay of PBA-labeled hen egg-white lysozyme is also triple exponential.[26] Finally, the Winnik group has reported that the time-resolved fluorescence intensity decays from pyrene-labeled (hydroxypropyl)celluloses are multiexponential.[15,27]

Considering the complexity of the dendrimer time-resolved intensity decay kinetics we have opted to use the mean fluorescence lifetimes $<\tau>$ (Table 1) to further assess the dendrimer photophysics. Inspection of the data presented in Table 1 shows that the trend in $<\tau>$ with dendrimer generation parallels the Φ_f and ϵ results, demonstrating that the pyrene residue is progressively shielded from the solvent as the dendrimer generation increases. From the Φ_f and $<\tau>$ data we calculated the average radiative (k_r) and nonradiative decay rates (k_{nr}) ($k_r = \Phi_f <\tau>^{-1}$; $k_{nr} = k_r(\Phi_f^{-1} - 1)$ for **P1**, **P2**, and **P3** dissolved in PB (Table 1). These results reveal the underlying reasons for the increase in Φ_f and, to a lesser extent $<\tau>$, as we proceed from **P1** to **P2** to **P3** we note the following: (1) a small (~13%) increase in k_r and (2) a 2-fold decrease in k_{nr}. Thus, the pyrenyl residue's nonradiative deactivation pathway is influenced significantly by the dendritic matrix; however, the radiative deactivation pathway is effectively independent of the dendrimer generation. Our research groups observed similar behavior for a series of dansyl-based dendrimers.[10]

Fluorescence Quenching of P*n*. Although radiative rates for an excited-state fluorescent species are generally insensitive to its molecular environment,[21,28,29] the efficiencies of nonradiative processes are strongly dependent upon perturbations caused by the presence of external agents such as quenchers. For example, excited-state pyrene is readily quenched by a host of molecules, ions, and atoms.[21,28,29] In homogeneous solutions the bimolecular quenching rate constants (k_q) that describe the pyrene/quencher system approach the diffusion limit ($k_q \sim 10^{10}\ M^{-1}\ s^{-1}$ in water at room temperature)[21]; however, the magnitude of k_q and even the quenching process itself can change significantly when pyrene is sequestered within organized assemblies such as micelles, vesicles, or membranes.[30−33] Thus, quencher studies can be used to provide additional information regarding the location or accessibility of intrinsic or extrinsic fluorophores within a macromolecular structure or conformational fluctuations therein.[33] In addition, by using a carefully selected set of quenching agents, one can discern the role of electrostatics and solute (quencher) type on the pyrene residue's accessibility as a function of dendritic branching.

The Stern−Volmer expression (eq 1) provides a link between the experimental measurables and the physical aspects of the quenching process:[21,33]

$$F_0/F = 1 + K_{SV}[Q] = 1 + <k_q> <\tau>_o[Q] \qquad (1)$$

In this expression F_0, F, K_{SV}, $<k_q>$, $<\tau>_0$, and $[Q]$ are the fluorescence intensity in the absence and presence of quencher, Stern−Volmer quenching constant, average bimolecular quenching constant, mean fluorophore lifetime in the absence of quencher, and the analytical concentration of quencher, respectively. In situations where the Stern−Volmer plots (F_0/F vs $[Q]$) are not linear, researchers have used a variety of more complex models.[21,33]

TABLE 3: Parameters Recovered from Fluorescence Quenching of P1, P2, and P3 by Various Quenching Agents

	P1		P2		P3	
	K_{SV} (M^{-1})	$<k_q>$ ($M^{-1}\,s^{-1}$)	K_{SV} (M^{-1})	$<k_q>$ ($M^{-1}\,s^{-1}$)	K_{SV} (M^{-1})	$<k_q>$ ($M^{-1}\,s^{-1}$)
CH_3NO_2	729.2 ± 11.0	$(5.66 \pm 0.14) \times 10^9$	552.3 ± 7.4	$(4.03 \pm 0.09) \times 10^9$	220.1 ± 9.4	$(1.53 \pm 0.07) \times 10^9$
$CH_2{=}CH\,CON\,H_2$	338.1 ± 4.2	$(2.62 \pm 0.06) \times 10^9$	253.2 ± 3.1	$(1.85 \pm 0.04) \times 10^9$	71.2 ± 1.0	$(0.49 \pm 0.01) \times 10^9$
$C_6H_5\,N(CH_3)_2$	804.7 ± 35.5	$(6.24 \pm 0.30) \cdot 10^9$	520.8 ± 20.8	$(3.80 \pm 0.17) \times 10^9$	127.4 ± 15.1	$(0.88 \pm 0.11) \times 10^9$
CH_3I	17.9 ± 2.1	$(1.39 \pm 0.17) \times 10^8$	10.0 ± 1.4	$(0.73 \pm 0.10) \times 10^8$	5.1 ± 0.9	$(0.35 \pm 0.06) \times 10^8$
KI	53.8 ± 2.5	$(4.17 \pm 0.21) \times 10^8$	22.1 ± 0.8	$(1.61 \pm 0.07) \times 10^8$	2.7 ± 0.1	$(0.19 \pm 0.08) \times 10^8$

Neutral Charge-Transfer Quenching. We initiate our discussion of the **P*n*** dendrimer quenching by using nitromethane (CH_3NO_2) and acrylamide ($CH_2{=}CHCONH_2$), both well-known, molecular charge-transfer quenchers.[33−36] During charge-transfer quenching, transfer of an electron (charge) takes place from the pyrene excited singlet state to the quencher with the formation of a transient charge-transfer complex. The Stern−Volmer plots for nitromethane and acrylamide quenching of the **P*n*** dendrimers are linear (nitromethane: $r^2 > 0.999$; acrylamide: $r^2 > 0.992$) and the K_{SV} and $<k_q>$ values are compiled in Table 3. Examination of these data shows a clear decrease in K_{SV} and $<k_q>$ as we proceed from **P1** to **P2** to **P3**. Specifically, an almost 4-fold decrease in $<k_q>$ is apparent between **P1** and **P3** quenched by nitromethane. Similarly, $<k_q>$ is more than five times lower for **P3** than for **P1** when quenched by acrylamide.The acrylamide bimolecular quenching rate for **P1** is less than half the diffusion-limited rate observed for tryptophan quenching in solution ($5.9 \times 10^9\ M^{-1}\,s^{-1}$).[33] In cases where quenchers can only access the fluorescent residue from a limited region (e.g., a fluorescently labeled protein where the protein partially blocks access to the fluorophore), the maximum k_q is expected to be less than the value for a purely diffusion-controlled reaction.[37] Our results on **P*n*** clearly suggest that: (1) even the lowest generation dendrimer, **P1**, effectively impedes quencher diffusion/access to the pyrenyl moiety and (2) the approach of neutral quenching agents toward the pyrenyl moiety is increasingly hindered as the dendrimer generation increases. We attribute this latter feature to the greater segmental density within the dendrimer network surrounding the pyrenyl moiety, with successive generation, that effectively impedes quencher access to the pyrenyl moiety (Figure 1). A similar effect was seen for a series of dansyl-based dendrimers complexing with cyclodextrins and anti-dansyl antibodies[10]; however, the size of the quenchers used in the current study are 10- to 1000-fold smaller than a cyclodextrin or anti-dansyl antibody, respectively. The lower $<k_q>$ seen for acrylamide relative to nitromethane can be rationalized by nitromethane's smaller van der Waals radius (1.7 vs 2.6 Å)[38] and thus higher diffusion coefficient. Finally, it is important to mention that the $<k_q>$ values observed here are all in good agreement with values reported previously[30,39] for these same quenchers when pyrene is located within microheterogeneous media and are always less than the diffusion-controlled limits.

Electron-transfer quenching of molecular fluorescence can occur when an electron is transferred from a donor species to an appropriate excited-state acceptor species. The *N,N′*-dimethylaniline (DMA)/pyrene system represents a classic case.[21,23,28,40−43] In nonpolar solvents, the excited-state complex (exciplex) resulting from intermolecular electron transfer from DMA to excited-state pyrene molecule manifests itself as a broad, low-energy, structureless band in the emission spectrum. However, in solvents with high dielectric constants, exciplex emission is not observed, because radical ions are formed with high efficiency from the electron-transfer quenching.[28] This phenomenon has been explained in terms of a dramatic increase in the probability of radiationless transitions.[28]

To better assess the effects of the dendrimer structure on quencher accessibility, we investigated the **P*n*** dendrimer fluorescence as a function of added DMA. In all cases, DMA quenching followed Stern−Volmer behavior ($r^2 > 0.990$) up to the DMA solubility limit in water.[11b] In parallel with our results for nitromethane and acrylamide, K_{SV} and $<k_q>$ for the **P*n***/DMA system decreases as we proceed from **P1** to **P2** to **P3** (Table 3) with a greater than 7-fold decrease in $<k_q>$ as the dendrimer generation is increased. By way of comparison the reported k_q values for the DMA/perylene system dissolved in several pure liquid solvents are $17.8 \times 10^9\ M^{-1}\,s^{-1}$ (acetonitrile), $8.0 \times 10^9\ M^{-1}\,s^{-1}$ (dimethylformamide), $1.9 \times 10^9\ M^{-1}\,s^{-1}$ (formamide), $12.2 \times 10^9\ M^{-1}\,s^{-1}$ (methanol), $1.5 \times 10^9\ M^{-1}\,s^{-1}$ (benzene), and $0.33 \times 10^9\ M^{-1}\,s^{-1}$ (methylcyclohexane).[28] Values of similar magnitude have also been reported for the pyrene/DMA system [$13 \times 10^9\ M^{-1}\,s^{-1}$ (acetonitrile),[23] $12 \times 10^9\ M^{-1}\,s^{-1}$ (acetonitrile),[44] and $4.5 \times 10^9\ M^{-1}\,s^{-1}$ (50:50 water/methanol, v/v)[23]]. We interpret the decrease in $<k_q>$ with increasing dendrimer generation to arise from the convolution of two factors. First, a decreased dipolarity within the cybotactic "pocket" in which the pyrenyl residue resides[10] giving rise to ever lower $<k_q>$ values from **P1** to **P2** to **P3**. Second, in line with the nitromethane and acrylamide results, the increased density afforded by the increasingly branched arboreal chains (Figure 1) effectively protects the excited pyrenyl residue from the approaching DMA molecules. No exciplex emission was observed for our **P*n***/DMA system in water.

Neutral Heavy-Atom Quenching. Another important class of molecular quenching agents exhibits external heavy-atom-quenching efficiencies that are roughly proportional to Z^4 where Z is the atomic number.[45−51] Quenchers of this type, as shown by Wilkinson and co-workers, quench fluorescence by enhancing intersystem crossing by spin−orbit coupling which is accompanied by a correspondingly enhanced triplet-state population.[49−51] Of course, singlet-to-triplet intersystem crossing may also be influenced by molecules containing heavy atoms as exemplified by the work of Quina and Carroll on alkylhalide quenching of polycyclic aromatic hydrocarbons.[52]

We explored the fluorescence quenching of our **P*n*** dendrimers by methyliodide (CH_3I), a neutral heavy-atom containing agent. The quenching of our **P*n*** dendrimers by CH_3I is well described by the Stern−Volmer expression ($r^2 > 0.982$). Although the K_{SV} for **P1** ($17.9\ M^{-1}$) is similar to the value reported for the anthracene/CH_3I system dissolved in cyclohexane ($18.8\ M^{-1}$),[28] Table 3 reveals the considerable shielding of the pyrenyl residue offered by the higher generation dendrimers. That is, although the smallest dendrimer (**P1**) offers minimal protection for the pyrenyl residue from CH_3I (by far

the smallest neutral solute/quencher used in this study), higher dendrimer generations offer a substantial diffusive barrier with $<k_q>$ values decreasing by a factor of about 4 between **P1** and **P3**. Thus, the molecular "netting" within **P3** is relatively impermeable to even small neutral quenchers/solutes such as CH_3I.

Charged Species Quenching. Because properties such as binding, solubility, and molecular recognition rely heavily on surface-charge effects, an understanding of such is essential to the rational design of dendrimer-based materials as efficient pharmaceutical vehicles, controlled release systems, reaction media, and the like. To assess the role of electrostatics in the molecular approach of charged quenchers/solutes toward a well-defined site within dendrimers of varying generation, we investigated the behavior of our **P*n*** dendrimers in the presence of the quenchers iodide (I^-) and cupric (Cu^{2+}) ions.

Like the behavior we saw with its neutral heavy atom counterpart, CH_3I, the I^--mediated quenching of our **P*n*** dendrimers follows a Stern−Volmer mechanism ($r^2 > 0.981$) with K_{SV} and $<k_q>$ that decrease with increasing generation number (Table 3). However, while $<k_q>$ decreases by a factor of 4 as we progress from **P1** to **P2** to **P3** for CH_3I, the $<k_q>$ for I^- systematically decreases more than 20-fold as we progress from **P1** to **P3**. Given that I^- is considerably smaller than CH_3I, electrostatics clearly play the dominant role in the observed **P*n*** dendrimer quenching behavior by I^-. To fully appreciate the subtleties of this process, it is important to realize that a large fraction of the surface carboxylic groups will be ionized at pH 7.0 (the acid dissociation constant for an isolated carboxylic acid K_a is 1.75×10^{-5}).[11c] On the basis of previous work from our groups on dansyl-based dendrimers,[10] we estimate the **P1**, **P2**, and **P3** hydrodynamic radii to be 5.7, 8.3, and 12.2 Å, respectively. Thus, considering that this series of dendrimers contains 3 (**P1**), 9 (**P2**), and 27 (**P3**) carboxylic acid groups in their peripheries, the surface-charge density is roughly twice as high for **P3** as it is for **P1**. At this point, it should be clear that in addition to the increased molecular crowding of the dendrimer chains surrounding the pyrenyl moiety (Figure 1), Coulombic repulsion is largely responsible for protection of the excited pyrenyl residue from I^- within **P3**. Provided merely as benchmarks, k_q values of 12.0×10^9 M^{-1} s^{-1} (acetonitrile), 8.0×10^9 M^{-1} s^{-1} (dimethylformamide), and 0.23×10^9 $M^{-1}s^{-1}$ (methanol) have been reported for perylene quenching by I^-.[28]

We now turn our attention to **P*n*** dendrimer quenching by Cu^{2+}, which acts as a heavy atom and electron scavenger,[21] both of which contribute to its quenching efficacy. (Note: It was necessary for us to perform the Cu^{2+}-quenching studies in distilled−deionized water to avoid Cu^{2+} precipitation by phosphate (vide supra).[11a] However, a large fraction of the dendrimer surface carboxylic acid groups should remain dissociated under these conditions.) As a benchmark, Thomas and co-workers[23] have reported that the k_q value for pyrene quenched by Cu^{2+} in water is 5.3×10^9 M^{-1} s^{-1}.

The Cu^{2+} quenching of our **P*n*** dendrimers proved to be complex (Figures 3−6). The results for the **P1**/Cu^{2+} system were characterized by a linear ($r^2 = 0.999$) Stern−Volmer plot (Figure 3). However, the recovered $<k_q>$ value (9.5×10^{10} M^{-1} s^{-1}) is about 20-fold *greater* than the k_q value for pyrene quenched by Cu^{2+} in water. This result suggests that charge-transfer and heavy-atom quenching are operating in concert with one or more additional quenching processes for the **P1**/Cu^{2+} system. In **P2** and **P3**, quenched by Cu^{2+} (Figures 4−6), the Stern−Volmer plots were nonlinear; the results for the higher generation

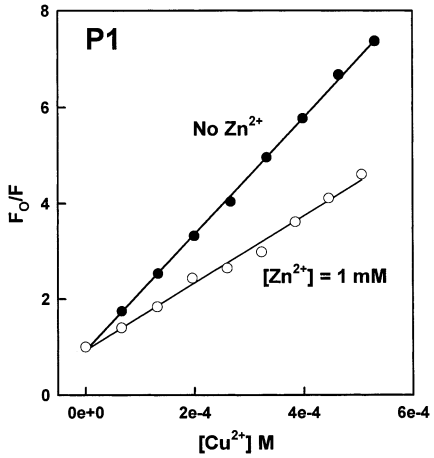

Figure 3. Stern−Volmer quenching plots for 1 μM **P1** by Cu^{2+} in the absence (closed symbols) and the presence of 1 mM Zn^{2+} (open symbols).

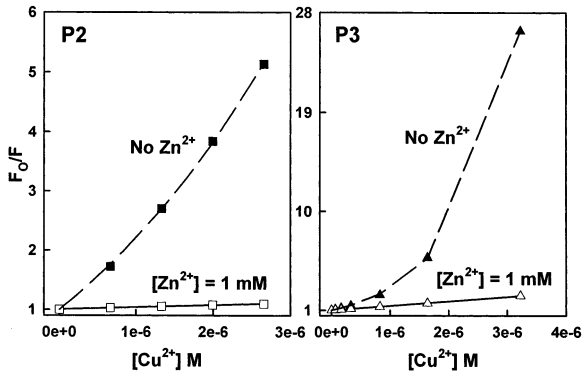

Figure 4. Stern−Volmer quenching plots (truncated quencher concentration range) for 1 μM **P2** and **P3** by Cu^{2+} in the absence (solid symbols) and presence of 1 mM Zn^{2+} (open symbols). Note that the plots without Zn^{2+} are nonlinear.

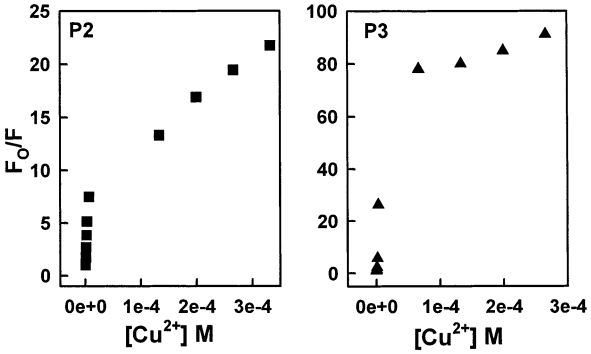

Figure 5. Stern−Volmer quenching plots (full range) for 1 μM **P2** and **P3** by Cu^{2+}. Note the quenching saturates at the higher Cu^{2+} concentrations and the plots are nonlinear.

dendrimers actually seem to saturate at the higher concentrations of Cu^{2+} investigated, and the Stern−Volmer plots are a function of the dendrimer analytical concentration (Figure 6). These results are fully consistent with Cu^{2+} binding to the **P*n*** dendrimers.[53−57]

At least two possible binding sites exist for cations within our dendrimers (Figure 1). First, one could envision electrostatic attraction and complexation between the dendrimer carboxylates and the Cu^{2+} quenchers that could bring the quenchers into the pyrenyl residue's immediate proximity on the **P*n*** dendrimer surface. A second possibility is the Cu^{2+} quenchers actually entering into and associating with parts of the dendrimer core

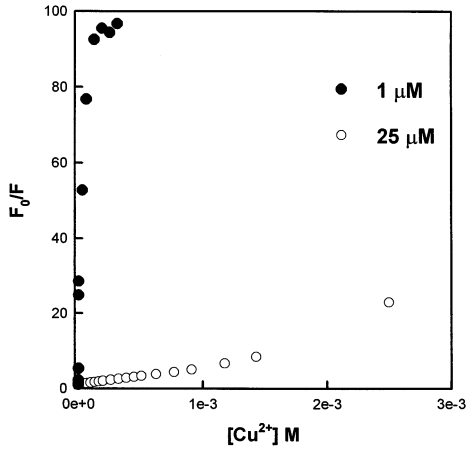

Figure 6. Effects of **P3** dendrimer concentration on the Stern−Volmer plot.

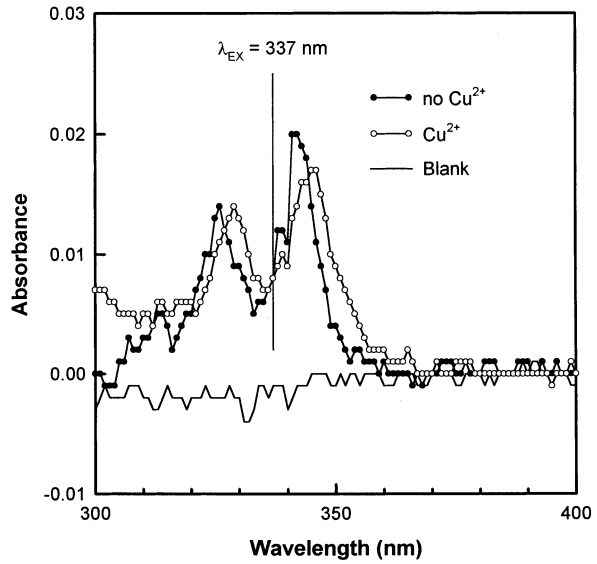

Figure 7. Electronic absorbance spectra for 1 μM **P3** in the absence and presence of 0.2 mM Cu^{2+}.

itself. It is well-known that Cu^{2+} has a particularly high thermodynamic affinity for typical N-,O-, and -S-based chelate ligands and fast metal-to-ligand binding kinetics.[53] In this context Okada's group demonstrated that Cu^{2+} associated with surface primary amines *and* internal tertiary amines in poly(l-glutamic acid).[54] Given this, it seems likely that Cu^{2+} could simultaneously coordinate within the skeleton of our dendrimers *and* bind to surface carboxylates which would increase the local concentration of Cu^{2+} surrounding the pyrenyl residue. The data in Figures 3−6 are consistent with these scenarios. Additional evidence for association/complexation is found in the dendrimer electronic absorbance spectra in the absence and presence of Cu^{2+} (Figure 7) where we note shifts in the absorbance spectra consistent with a static, ground-state complex.

In an electrolyte, Coulombic interactions can be screened by free ions.[58] Thus, addition of an excess of a second divalent cation (e.g., Zn^{2+} added as $ZnSO_4$) to our system should screen the surface charge on the dendrimer resulting in reduced electrostatic attraction by Cu^{2+} and concomitantly reduced quenching (Zn^{2+} itself is not a molecular quencher of pyrene[28]). The results in Figures 3 and 4 show that addition of a 1000:1 mole ratio of Zn^{2+}:dendrimer reduces the extent of Cu^{2+} quenching. However, the recovered $<k_q>$ values, even in the presence of 1 mM Zn^{2+}, are at least a factor of 10 (for **P1**) and up to a factor of 500 (for **P3**) greater than predicted for a diffusion-controlled reaction. Thus, the addition of excess Zn^{2+} (1000-fold over the concentration of dendrimer) can decrease the amount of Cu^{2+} bound to the dendrimers, but it does not eliminate the Cu^{2+} binding. The exact nature of the Cu^{2+} association to and quenching of these **P*n*** dendrimers is unknown and currently under investigation in our laboratories.

Conclusions

By using pyrene as a spectroscopic probe sensitive to a series of water-soluble quenchers, we have evaluated several aspects of the local morphology and accessibility within a family of poly(amido) carboxylate dendrimers (Figure 1). Fluorescence quantum yields and, to a lesser extent, excited-state fluorescence lifetimes of the pyrenyl moiety increase and molar absorptivities decrease as the dendrimer generation increases. This behavior is largely a consequence of a decrease in the nonradiative decay rate with increasing dendrimer generation. Approach of neutral (nitromethane, acrylamide, *N*,*N*′-dimethylaniline, and methyl iodide) and anionic (iodide ion) fluorescence-quenching agents toward the pyrenyl moiety is increasingly hindered with dendrimeric generation. This effect is, however, markedly more dramatic for the anionic quencher because electrostatic repulsion between the anionic quencher and anionic dendrimer surface increases as *n* increases. The quenching of our **P*n*** dendrimers by Cu^{2+} do not follow any of the basic quenching models, small amounts of quencher ($\ll$1 mM) can lead to near total quenching of the fluorescence, and the apparent quenching rates are orders of magnitude greater than is possible for a diffusion-controlled reaction. We attribute these results to association of the Cu^{2+} with our dendrimers. The quenching results with Cu^{2+} also suggest the potential of using these types of dendrimers as amplifiers for sensing divalent metal cations that can quench the pyrene residue fluorescence.

Acknowledgment. The authors thank the American Chemical Society for an Analytical Division Fellowship sponsored by Eli Lilly (G.A.B.), the National Institutes of Health for a Minority Graduate Fellowship (C.M.C.), the National Science Foundation (to A.E.K., CHE-9982014; and to F.V.B., CHE-0078101), the Department of Energy (to F.V.B), and the University at Buffalo (to F.V. B.).

References and Notes

(1) For recent reviews, see: (a) Chow, H.-F.; Mong, T. K.-K.; Nomgrum, M. F.; Wan, V. W. *Tetrahedron* **1998**, *54*, 8543. (b) Newkome, G. R.; He, E.; Moorefield, C. N. *Chem. Rev.* **1999**, *99*, 1689. (c) Archut, A.; Vögtle, F. *Chem. Soc. Rev.* **1999**, *27*, 233. (d) Hecht, S.; Fréchet, J. M. *Angew. Chem., Int. Ed. Engl.* **2001**, *40*, 74.

(2) (a) Kalyanasundaram, K. In *Photochemistry in Organized and Constraint Media*; Ramamurthy, V., Ed.; VCH: Weinheim, 1991; p 39. (b) Carmichael, I.; Hug, G. L. *Handbook of Photochemistry*, 2nd ed.; Marcel Dekker: New York, 1993.

(3) (a) Pistolis, G.; Malliaris, A.; Paleos, C. M.; Tsiourvas, D. *Langmuir* **1997**, *13*, 5870. (b) Pistolis, G.; Malliaris, G.; Tiourvas, D.; Paleos, C. M. *Chem. Eur. J.* **1999**, *5*, 1440.

(4) Frank, R. S.; Merkle, G.; Gauthier, M. *Macromolecules* **1997**, *30*, 5397.

(5) Baker, L. A.; Crooks, R. M. *Macromolecules* **2000**, *33*, 9034.

(6) Riley, J. M.; Alkan, S.; Chen, A.; Shapiro, M.; Khan, W. A.; Murphy, W. R.; Hanson, J. E. *Macromolecules* **2001**, *34*, 1797.

(7) Hecht, S.; Vladimirov, N.; Fréchet, J. M. J. *J. Am. Chem. Soc.* **2001**, *123*, 18.

(8) Newkome, G. R.; Behera, R. K.; Moorefield, C. N.; Baker, G. R. *J. Org. Chem.* **1991**, *26*, 4376.

(9) Cardona, C. M.; McCarley, T. D.; Kaifer, A. E. *J. Org. Chem.* **2000**, *65*, 1857.

(10) Cardona, C. M.; Alvarez, J.; Kaifer, A. E.; McCarley, T. D.; Pandey, S.; Baker, G. A.; Bonzagni, N. J.; Bright, F. V. *J. Am. Chem. Soc.* **2000**, *122*, 6139.

(11) Dean, J. A. *Lange's Handbook of Chemistry*, 14th ed.; McGraw-Hill: New York, 1992; (a) Table 8.6, (b) Table 1.15, (c) Table 8.8.
(12) Mardelli, M.; Olmsted, J. *J. Photochem.* **1977**, *7*, 277−285.
(13) Lakowicz, J. R.; Weber, G. *Biochemistry* **1973**, *12*, 4161.14.
(14) Hara, K.; Ware, W. R. *Chem. Phys.* **1980**, *51*, 61.
(15) Winnik, F. M.; Winnik, M. A.; Tazuke, S.; Ober, C. K. *Macromolecules* **1987**, *20*, 38.
(16) Parker, C. A.; Rees, W. T. *Analyst* **1962**, *87*, 83.
(17) Murov, S. L.; Carmichael, I.; Hug, G. L. *Handbook of Photochemistry*, 2nd ed.; Marcel Dekker: New York, 1993; p 44.
(18) Karpovich, D. S.; Blanchard, G. J. *J. Phys. Chem.* **1995**, *99*, 3951.
(19) Naciri, J.; Weiss, R. G. *Macromolecules* **1989**, *22*, 3928.
(20) Winnik, M. A.; Bystryak, S. M.; Liu, Z.; Siddiqui, J. *Macromolecules* **1998**, *31*, 6855.
(21) Lakowicz, J. R. *Principles of Fluorescence Spectroscopy*, 2nd ed.; Kluwer Academic/Plenum Publishers: New York, 1999.
(22) Vethamuthu, M. S.; Almgren, M.; Mukhtar, E.; Bahadur, P. *Langmuir* **1992**, *8*, 2396.
(23) Hashimoto, S.; Thomas, J. K. *J. Colloid Interface Sci.* **1984**, *102*, 152.
(24) De Feyter, S.; van Stam, J.; Boens, N.; De Schryver, F. C. *Chem. Phys. Lett.* **1996**, *249*, 46.
(25) Ishiji, T.; Kaneko, M. *Analyst* **1995**, *120*, 1633.
(26) Pan, B.; Berglund, K. A. *J. Crystal Growth* **1997**, *171*, 226.
(27) Yamazaki, I.; Winnik, F. M.; Winnik, M. A.; Tazuke, S. *J. Phys. Chem.* **1987**, *91*, 4213.
(28) Birks, J. B. *Photophysics of Aromatic Molecules*; Wiley-Interscience: London, 1970.
(29) Turro, N. J. *Modern Molecular Photochemistry*; University Science Books: Sausalito, CA, 1991.
(30) Chen, T. S.; Thomas, J. K. *J. Polym. Sci.*: *Polym. Chem. Ed.* **1979**, *17*, 1103.
(31) Gratzel, M.; Thomas, J. K. In *Modern Fluorescence Spectroscopy*; Wehry, E. L., Ed.; Plenum Press: New York, 1974; Vol. 2.
(32) Thomas, J. K. *Acc. Chem. Res.* **1977**, *10*, 133.
(33) Eftink, M. R. In *Topics in Fluorescence Spectroscopy*; Lakowicz, J. R., Ed.; Plenum Press: New York, 1991; Vol. 2; see also references therein.
(34) Acree, W. E., Jr.; Pandey, S.; Tucker, S. A. *Curr. Top. Solution Chem.* **1997**, *2*, 1.
(35) Zander, M. In *Chemical Analysis of Polycyclic Aromatic Compounds*; Vo-Dinh, T., Ed.; John Wiley: New York, 1989.
(36) Acree, W. E., Jr.; Pandey, S.; Tucker, S. A.; Fetzer, J. C. *Polycyclic Aromat. Compd.* **1997**, *12*, 71.
(37) Johnson, D. A.; Yguerabide, J. *Biophys. J.* **1985**, *48*, 949.
(38) Semiempirical calculations were carried out with HyperChem 4.5 (Hypercube Inc.) using PM3-optimized geometries.
(39) Thomas, J. K. *Chem. Rev.* **1980**, *80*, 283; see also references therein.
(40) Okamoto, M. *J. Phys. Chem. A.* **2000**, *104*, 5029; see also references therein.
(41) Herbrich, R. P.; Schmidt, R. *J. Photochem. Photobiol. A* **2000**, *133*, 149.
(42) Mataga, N.; Ezumi, K.; Okada, T. *Mol. Phys.* **1966**, *10*, 203.
(43) Schomburg, H.; Staerk, H.; Weller, A. *Chem. Phys. Lett.* **1973**, *22*, 1.
(44) Taylor, G. N.; Chandross, E. A.; Shiebel, A. H. *J. Am. Chem. Soc.* **1974**, *96*, 2693.
(45) Kasha, M. *J. Chem. Phys.* **1952**, *20*, 71.
(46) McGlynn, S. P.; Reynolds, M. J.; Daigre, G. W.; Christodouleas, N. D. *J. Phys. Chem.* **1962**, *66*, 2499.
(47) McGlynn, S. P.; Azumi, T.; Kinoshita, M. *Molecular Spectroscopy of the Triplet State*; Prentice Hall: Englewood Cliffs, NJ, 1969.
(48) McGlynn, S. P.; Azumi, T.; Kasha, M. *J. Chem. Phys.* **1964**, *40*, 507.
(49) Medinger, T.; Wilkinson, F. *Trans. Faraday Soc.* **1965**, *61*, 620.
(50) Horrocks, A. R.; Wilkinson, F. *Proc. R. Soc. London Ser. A* **1968**, *306*, 257.
(51) Wilkinson, F. *Adv. Photochem.* **1964**, *3*, 241.
(52) Quina, F. H.; Carroll, F. A. *J. Am. Chem. Soc.* **1976**, *98*, 6.
(53) For copper ion complexation by poly(amidoamine) dendrimers, see: (a) Zhou, L.; Russell, D. H.; Zhao, M.; Crooks, R. M. *Macromolecules* **2001**, *34*, 3567. (b) Zhao, M.; Sun, L.; Crooks, R. M. *J. Am. Chem. Soc.* **1998**, *120*, 4877. (c) Zhao, M.; Crooks, R. M. *Angew. Chem., Int. Ed. Engl.* **1999**, *38*, 364. (d) Balogh, L.; Tomalia, D. A. *J. Am. Chem. Soc.* **1998**, *120*, 7355. (e) Swager, T. M. *Acc. Chem. Res.* **1998**, *31*, 201.
(54) Tsutsumiuchi, K.; Aoi, K.; Okada, M. *Polym. J.* **2000**, *32*, 107.
(55) Wang, J.; Wang, D.; Miller, E. K.; Moses, D.; Bazan, G. C.; Heeger, A. J. *Macromolecules* **2000**, *33*, 5153.
(56) Blatt, E.; Sawyer, W. H. *Biochim. Biophys. Acta* **1985**, *822*, 43.
(57) Blatt, E.; Chatelier, R. C.; Sawyer, W. H. *Biophys. J.* **1986**, *50*, 349.
(58) Israelachvili, J. In *Intermolecular & Surface Forces*, 2nd ed.; Academic Press Inc.: San Diego, 1991.